Real-time forecasting of the April 11, 2012 Sumatra tsunami

Dailin Wang,[1] Nathan C. Becker,[1] David Walsh,[1] Gerard J. Fryer,[1] Stuart A. Weinstein,[1] Charles S. McCreery,[1] Victor Sardiña,[1] Vindell Hsu,[1] Barry F. Hirshorn,[1] Gavin P. Hayes,[2] Zacharie Duputel,[3] Luis Rivera,[4] Hiroo Kanamori,[3] Kanoa K. Koyanagi,[1] and Brian Shiro[1]

Received 13 July 2012; revised 24 August 2012; accepted 24 August 2012; published 2 October 2012.

[1] The April 11, 2012, magnitude 8.6 earthquake off the northern coast of Sumatra generated a tsunami that was recorded at sea-level stations as far as 4800 km from the epicenter and at four ocean bottom pressure sensors (DARTs) in the Indian Ocean. The governments of India, Indonesia, Sri Lanka, Thailand, and Maldives issued tsunami warnings for their coastlines. The United States' Pacific Tsunami Warning Center (PTWC) issued an Indian Ocean-wide Tsunami Watch Bulletin in its role as an Interim Service Provider for the region. Using an experimental real-time tsunami forecast model (RIFT), PTWC produced a series of tsunami forecasts during the event that were based on rapidly derived earthquake parameters, including initial location and Mwp magnitude estimates and the W-phase centroid moment tensor solutions (W-phase CMTs) obtained at PTWC and at the U. S. Geological Survey (USGS). We discuss the real-time forecast methodology and how successive, real-time tsunami forecasts using the latest W-phase CMT solutions improved the accuracy of the forecast. **Citation:** Wang, D., et al. (2012), Real-time forecasting of the April 11, 2012 Sumatra tsunami, *Geophys. Res. Lett.*, *39*, L19601, doi:10.1029/2012GL053081.

1. Introduction

[2] U.S. Tsunami Warning Centers (TWCs) generally issue their tsunami warnings based on initial earthquake magnitude and calculated tsunami travel times. The TWCs also utilize two pre-computed databases of tsunami scenarios to provide a quick estimate of possible tsunami threat for some specific points and areas of interest: the Short-term Inundation Forecasting for Tsunamis (SIFT) database forecast method [*Gica et al.*, 2008] and the Alaska Tsunami Forecast Model (ATFM) [*Kowalik and Whitmore*, 1991; *Kowalik et al.*, 2005]. The ATFM forecast method has nested coastal grids and has the capability to scale forecasts to sea level observations. SIFT has the capability of using observations from deep ocean bottom pressure sensors (DARTs) to constrain the propagation database models by combining pre-computed unit-source solutions to best match observations (DART-inversion). Inundation models can then be run in real-time, using the propagation solution as initial and boundary conditions to refine the tsunami forecasts [*Wei et al.*, 2008].

[3] The U.S. database methods have some limitations, however. For example, these methods only model tsunamigenic earthquakes located in known subduction zones. All the sources in the database are of the pure thrust type. Nature sometimes violates this assumption. Recent non-thrust tsunamigenic earthquakes have included the Kuril 2007 (Mw = 8.1, normal faulting), Samoa 2009 (Mw = 8.0, normal and thrust faulting), and Sumatra 2012 (Mw = 8.6, 8.2, strike-slip faulting) events. Furthermore, the finite number of pre-computed sources in the databases cannot exhaust all possible earthquake foci and the unit-sources are too large to accurately represent smaller earthquakes. We should point out that Japan Meteorological Agency's database tsunami forecast system contains more sources than in the U.S. system, including scenarios with normal-faulting and strike-slip faulting [*Tatehata*, 1997; *Kamigaichi*, 2009]. In their current implementation these pre-computed database models are confined to specific ocean basins and cannot be used to forecast inter-oceanic tsunamis, such as the 2004 Indian tsunami. It is therefore highly desirable for the TWCs to have in addition the capability to forecast tsunamis in real-time for earthquakes in any location with any focal mechanism using rapidly derived earthquake parameters. A real-time model can also forecast tsunamis that would be impossible to forecast with the database approach, including tsunamis generated by non-seismic events such as landslides, asteroid impacts, or meteorological forcing.

[4] Driven primarily by these operational needs, PTWC developed an experimental real-time tsunami forecast model (RIFT), to complement the pre-computed database approach [*Wang et al.*, 2009; *Fryer et al.*, 2010; *Foster et al.*, 2012]. The RIFT model also has a built-in simple slump landslide model. Other sources such as asteroid impact or meteorological forcing will be added in the future. TWC duty scientists can use the RIFT model to obtain an initial tsunami forecast in a matter of seconds using a default focal mechanism or a historical centroid moment tensor (CMT) solution. The RIFT model also capitalizes on recent developments in seismology, such as the rapid W-phase method [*Kanamori and Rivera*, 2008; *Hayes et al.*, 2009; *Duputel et al.*, 2011, 2012], which can compute a CMT for an earthquake only 20–30 minutes after the origin time. The duty scientists can then re-run the model to update the forecast with a W-phase solution as soon as one becomes available. The April 11, 2012 Sumatra tsunami put the RIFT model to the test and demonstrated that successive forecasts using the

[1]Pacific Tsunami Warning Center, NWS, NOAA, Ewa Beach, Hawaii, USA.
[2]National Earthquake Information Center, U.S. Geological Survey, Golden, Colorado, USA.
[3]Seismological Laboratory, California Institute of Technology, Pasadena, California, USA.
[4]Institut de Physique Globe de Strasbourg, UMR 7516 CNRS, UdS/EOST, Strasbourg, France.

Corresponding author: D. Wang, Pacific Tsunami Warning Center, NWS, NOAA, 91-270 Fort Weaver Rd., Ewa Beach, HI 96706, USA. (dailin.wang@noaa.gov)

latest W-phase CMT solutions improved the accuracy of the forecasts.

2. Methodology

[5] The RIFT model is based on the finite difference discretization of the linear shallow-water equations,

$$\boldsymbol{u}_t + \boldsymbol{f} \times \boldsymbol{u} = -g\nabla\eta, \tag{1}$$

$$\eta_t + \nabla \cdot (\boldsymbol{u}H) = 0, \tag{2}$$

where $\boldsymbol{u} = (u,v)$ is the vertically averaged horizontal velocity, $\boldsymbol{f}$ the Coriolis parameter, g the gravitational acceleration, η the sea surface elevation (deviation from the mean sea-level), H the ocean depth at rest, and ∇ the horizontal gradient operator. The model is cast in the spherical coordinates, with a leapfrog time differencing scheme on an Arakawa C-grid [*Arakawa and Lamb*, 1977], similar to the schemes used in *Imamura* [1996] except that simple leap-frog time difference scheme is used, instead of the staggered leap-frog scheme.

[6] The initial condition is based on the static seafloor deformation formula of *Okada* [1985] for a rectangular fault, with a shear modulus of 45 GPa and a Poisson ratio of 0.25. The fault size is a continuous function of earthquake magnitude, defined by the empirical formulae of *Wells and Coppersmith* [1994]. Although subduction earthquakes were excluded in their analysis, the formulae for fault length are in general agreement with the findings of *Henry and Das* [2001] (within 10–15%). The top of the fault has a minimum depth of 5 km. Namely, if the input fault depth causes the top of the fault to intersect the seafloor, it is adjusted such that the top of the fault is 5 km beneath the seafloor. A uniform slip, computed from moment, fault size, and shear modulus is used.

[7] For the focal mechanism input, we employ a hierarchy of approaches. As soon as an estimate of earthquake location and a magnitude is available (but before a CMT solution is available), the model determines an *a priori* focal mechanism by assuming a thrust, normal, or strike-slip mechanism based on the epicenter's proximity to convergent, divergent, or transform plate boundaries, respectively. We use the coordinates of the plate boundaries compiled by the U. S. Geological Survey (USGS) (see http://earthquake.usgs.gov/regional/nca/virtualtour/kml/Earths_Tectonic_Plates.kmz). To be conservative, the default focal mechanism for the initial forecast can be assumed to be a pure thrust, even if the earthquake occurred near a transform plate boundary. RIFT can also choose the focal mechanism from one of the more than 25,000 centroid moment tensor (CMT) solutions available in the Global CMT Project's catalog (http://www.globalcmt.org). As a W-phase CMT, USGS CMT, or quick Global CMT solutions becomes available, the model can be run again to generate a forecast using the most recently computed focal mechanism.

[8] For every model coastal grid point (wet-point), we determine wave amplitude by applying Green's Law [*Lamb*, 1932],

$$A_c = A_o(H_o/H_c)^{1/4}, \tag{3}$$

where A_c and A_o represent wave amplitudes at a coastal point (model coastal wet-point, or the first ocean grid point away from land) and a corresponding offshore point, respectively; H_c and H_o are water depths at the same coastal point and the offshore point, respectively. The offshore point is the closest model grid point to the coastal wet-point but with a water depth $H_o \geq H_d$, where H_d is defined as

$$H_d = \frac{1}{g}(8\Delta x/P)^2, \tag{4}$$

where Δx is the grid size, and P = 10 min. Equation (4) states that for a given grid size Δx, waves with a 10-min. period can be resolved (implying that there are a minimum of eight grid points per wave length) if the water depth is equal or greater than H_d. In other words, the offshore wave amplitude in Green's law must be derived from resolvable waves. At 30-arc-sec resolution, H_d = 15.5 m, which means the offshore point can be very close to the actual coastal point. At 4-arc-min. resolution, H_d = 992 m. Green's Law applies to linear coastlines exposed to the open ocean, in the absence of significant wave reflection, breaking, and dissipation. We choose H_c = 1 m for every coastal point. Since coastal sea-level stations are usually in locations with water depths greater than 1 m, the Green's Law amplitude should be a conservative estimate if there are no mitigating factors. The choice of H_c is not a major problem for tsunami warning purposes, because Green's Law amplitudes are rather insensitive to the choice of H_c. For example, the difference in A_c between H_c = 1 m and H_c = 10 m is only a factor of 1.77. To take account of the detailed geometry of specific locations (e.g., harbors inside lagoons or resonant harbors that historically tend to exhibit amplification of tsunamis), an empirical Green's Law for each location can be used. For example, *Reymond et al.* [2012] adopted a slope-dependent modifying factor of A_o in (3), to take into account the specific response of each sea level station. Such a practice is not feasible, however, for every coastal point on the model grid due to lack of historical tsunami data.

[9] For bathymetry, we use the GEBCO 30-arc-sec data [*Becker et al.*, 2009]. The RIFT model domain options include 40 predefined ocean basins, encompassing all the world's ocean basins and major marginal seas. The operator can also manually specify the model domain size, resolution, and integration length. The default model domain covers a region within four hours tsunami travel time from the earthquake as determined on-demand by the tsunami travel-time software [*Wessel*, 2009]. A forecast for this default model domain can be obtained in about 10 seconds at 4-arc-min. resolution on an 8-CPU Linux server. For smaller earthquakes (magnitudes <7.5), especially those occurring in isolated regions, the model domain can be smaller than defined by the 4-hour tsunami travel time and finer resolutions can be used. For earthquakes in Hawaii, for example, a tsunami forecast for the entire State at 30-arc-resolution can be obtained in 15 seconds. For very large earthquakes, once a solution is obtained for regions within four hours of tsunami travel time, a larger domain run can be started. A 26-hour forecast for the entire Pacific basin at 4-arc-min. resolution, including 15,000 coastal points can be obtained in less than seven minutes. An 18-hour forecast for the Indian Ocean takes about two minutes to complete. A global domain

Table 1. Timeline of Events at PTWC and Parameters Used in Real-Time Forecast

Time (GMT)	Events	Parameters/Comments
08:39Z	Mw = 8.6 earthquake origin time	Lat = 2.3°N, Lon = 93.1°E, Depth = 23 km] (USGS final location)
08:44Z	PTWC Issues Observatory Message, Mwp = 8.7	
08:44Z	Automated RIFT forecast for regions within 2500 km radius of the epicenter. Solution No. 1 (SOL1)	Preliminary earthquake parameters, Mw = 8.80, Assuming shallow thrust mechanism. Lat = 1.9°N, Lon = 92.5°E, depth = 33 km, Strike = 60°, Dip = 15°, Rake = 90° , Fault-length L = 483 km, Fault-width W = 100 km
08:45Z	PTWC issues Indian Ocean Basin-wide Tsunami Watch	
08:52 Z	RIFT forecast for the Indian Ocean. Solution No. 2 (SOL2)	Refined earthquake parameters Assuming shallow thrust Mw = 8.66 Lat = 2.4°N, Lon = 93.1°E, depth = 33 km, Strike = 319°, Dip = 15°, Rake = 90°, L = 400 km, W = 87 km
09:01Z	USGS W-phase CMT solution	Mw = 8.60
09:02Z	PTWC W-phase CMT solution	Mw = 8.78
09:17Z	RIFT forecast for the Indian Ocean Solution No. 3 (SOL3)	PTWC W-phase CMT, Mw = 8.78 Lat = 2.1°N, Lon = 92.2°E, Depth = 12 km Strike = 202°, Dip = 29°, Rake = 7°, L = 747 km, W = 40.8 km
09:23Z	USGS updated W-phase CMT	Mw = 8.57
10:16Z	RIFT forecast for the Indian Ocean Solution No. 4 (SOL4)	USGS W-phase CMT, Mw = 8.57 Lat = 2.3°N, Lon = 92.9°E, Depth = 25 km Strike = 199°, Dip = 80°, Rake = 3°, L = 544 km, W = 36 km
10:43Z	Magnitude 8.2 earthquake occurs	Lat = 0.8°N, Lat = 92.5°E, Depth = 16 km
12:36Z	PTWC cancels tsunami watch	sea-level observations confirmed no significant waves were observed from the 2nd EQ

run can also be performed if the situation warrants; a 48-hour global forecast takes 50 minutes.

3. April 11, 2012 Sumatra Tsunami

[10] At 08:39 UTC, April 11, 2012, a magnitude 8.6 earthquake occurred off the northern coast of Sumatra at (2.3°N, 93.1°E, see USGS's website for details of the earthquake: http://earthquake.usgs.gov/earthquakes/recenteqsww/Quakes/usc000905e.php#details), followed by a magnitude 8.2 earthquake 180 km to the south approximately two hours later. Tsunami warnings were issued by the governments of India, Indonesia, Sri Lanka, Thailand, and Maldives. The Pacific Tsunami Warning Center (PTWC) issued an Indian Ocean-wide Tsunami Watch Bulletin. RIFT was run multiple times during the event, using the latest earthquake parameters at the time. Although the RIFT model can handle multiple earthquakes with different origins, it was not run for the second earthquake because the magnitude was smaller than the first and because it was further from the trench than the first event, suggesting that it possibly had similar focal mechanism to the first (later confirmed by the Global CMT solution). Table 1 shows the timeline of events related to the earthquake response at PTWC and the parameters used in RIFT's forecasts. Approximately 5 minutes after the earthquake origin time, PTWC issued an observatory message, reporting the preliminary earthquake parameters to the USGS and various seismological observatories and organizations. Just before PTWC issued the first Tsunami Watch Bulletin, a RIFT forecast for a regional domain was obtained at 08:44Z or 6-min. after the origin (Figure 1a, solution no. 1 or SOL1). At the time, the magnitude was 8.8, different from 8.7 in the observatory message, due to round off. Although the epicenter is closer to a region characterized by strike-slip type earthquakes, a shallow thrust focal mechanism was assumed (strike = 60°, dip = 15°, rake = 90°), to be conservative. The results indicated there could be a significant tsunami (wave amplitude > 2 m) for regions near the epicenter, including Indonesia, Sri Lanka, and Northwest Australia. We should point out the strike = 60° (or 240° = 60° + 180°) used is different from the orientation of the Sunda Trench, which has a strike of 319° near this location, similar to the ones in the SIFT database. If a strike-slip focal mechanism were used, the results would have been much closer to reality, as a post-event run showed. In other words, a significant tsunami was not generated.

[11] After the basin-wide Tsunami Watch Bulletin was issued at 08:45 UTC, RIFT was run again for the entire Indian Ocean (at 4-arc-min. resolution), using refined earthquake parameters (SOL2, obtained at 08:52 UTC). Because the refined location was closer to the Sunda Trench than was the preliminary solution, the trench-strike-parallel nodal plane of the default mechanism was used (strike = 319°), assuming a shallow thrust focal mechanism (dip = 15°, rake = 90°). The results indicated this could be a major basin-crossing tsunami. Figure 1b shows the predicted maximum wave. Not surprisingly, this result was similar to the result obtained during the event using the SIFT database model as it used a similar assumed source (not shown).

[12] At 09:01 UTC (23 min. after the origin), the USGS distributed a preliminary W-phase CMT solution (Mw = 8.6) to various organizations, including PTWC. From 09:02 UTC to 09:10 UTC, four additional W-phase CMT solutions were computed by PTWC. The last W-phase CMT of the four was used in the RIFT forecast no. 3 obtained at 09:17 UTC (SOL3, Figure 1c). This solution, showing more strike-slip than thrust character, indicated the earthquake would not generate a significant tsunami, except near the epicenter or possibly in Sri Lanka, despite the fact that the magnitude

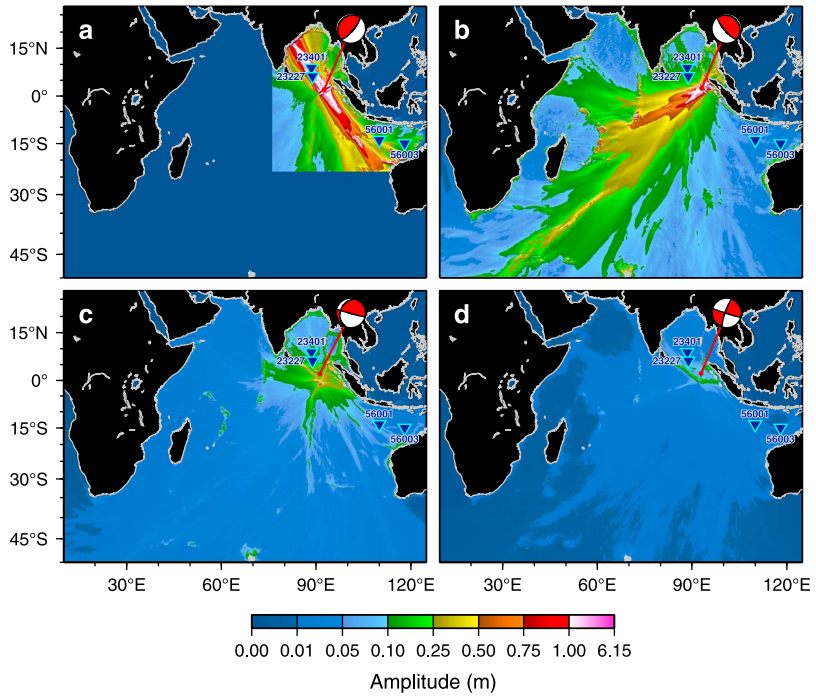

Figure 1. RIFT forecasts during the April 2012 Sumatra tsunami event: maximum wave amplitude for a regional domain (a) SOL1, thrust mechanism, at 08:44Z; (b) SOL2, thrust, at 08:52Z, (c) SOL3, PTWC's W-phase CMT, at 09:17Z, and (d) SOL4, USGS's final W-phase CMT, at 10:16Z. Inverted triangles indicate the locations of DART sensors. Focal mechanisms indicate those used to generate the RIFT forecast in each case. Note the dramatic differences in energy patterns between different runs. Wave amplitude is defined as an average of maximum zero to peak and zero to trough amplitudes. The map was created using the Generic Mapping Tool (GMT) by *Wessel and Smith* [1991].

used was actually larger than in SOL2 (8.78 vs. 8.66). It is worth noting that such a result cannot be anticipated from the database approach because the magnitude effectively determines the size of the tsunami. Using sea-level observations for inversion in a database model could be an attempt to fit those observations to the incorrect assumed thrust mechanism and subduction zone location (note that the nearest two DARTs has an azimuthal gap of 347 relative to the epicenter). This limitation inherent to database models illustrates the importance of having a real-time tsunami forecasting capability using the latest earthquake parameters for tsunami warning.

[13] At 10:16 UTC, RIFT was run again for the Indian Ocean (solution no. 4 or SOL4), using the final USGS W-phase CMT solution (primary nodal plane), which was posted online at 09:23 UTC. This focal mechanism indicated an almost pure strike-slip event. For this region, it is not obvious which CMT nodal plane should be used. The initial aftershocks within the first hour of the main shock however, favor the primary nodal plane, which we chose. Because of the smaller magnitude and steeper dip angle, the maximum wave amplitude was smaller than in SOL3 (Figure 1d). Based upon the computed focal mechanism, RIFT forecast, that the epicenter was clearly not in the subduction zone, and the small-amplitude tsunami waves observed so far, duty scientists at PTWC were increasingly confident that this earthquake had not generated a major tsunami.

[14] Four active Indian Ocean DARTs recorded the tsunami: DART buoys 23227, 23401, 56001, and 56003. Figure 2a compares wave amplitudes from RIFT forecasts with these observations. Results from a post-event run using the USGS W-phase CMT conjugate nodal plane are also included for comparison (SOL5, green bars). SOL1 dramatically overestimated the DART response (more than one meter, not shown). Despite the dramatic differences in the overall wave energy propagation (Figure 1), solutions obtained at 09:17 UTC (SOL2, blue) and at 10:16 UTC (SOL3, cyan) are rather similar at the four DARTs. Both solutions substantially overestimated the wave amplitude compared to observations (black). The agreement between SOL4 (strike-slip) and observations is much better, although the predicted wave amplitude is about half that observed at DART 23401. If a smaller fault length and a shallower depth were used, the results would have been much better, as post-event tests showed. Still, the simple rectangular fault with a uniform slip may be too simplistic. The next level sophistication of real-time tsunami forecast might be using the distributed slip approach of *Geist and Dmowska* [1999] and *Geist* [2005]. In the future, DART inversion using real-time RIFT model runs with subfaults on the CMT nodal planes might further improve the forecast accuracy. Sea-level stations across the Indian Ocean recorded the tsunami, as far as 4800 km from the epicenter, at Rodrigues Island. Figure 2b compares the predicted Green's Law wave amplitudes to observations at fourteen sea-level stations. Despite the similarities of SOL2 and SOL3 at the DARTs, the wave amplitudes at sea-level stations are very different. SOL3 shows considerably smaller wave amplitudes for most of the sea-level stations. The solution from USGS's final W-phase CMT (SOL4) showed the best agreement in all cases, correctly predicting that the wave amplitudes at sea-level stations would be below 1 m. With hindsight, SOL5 should

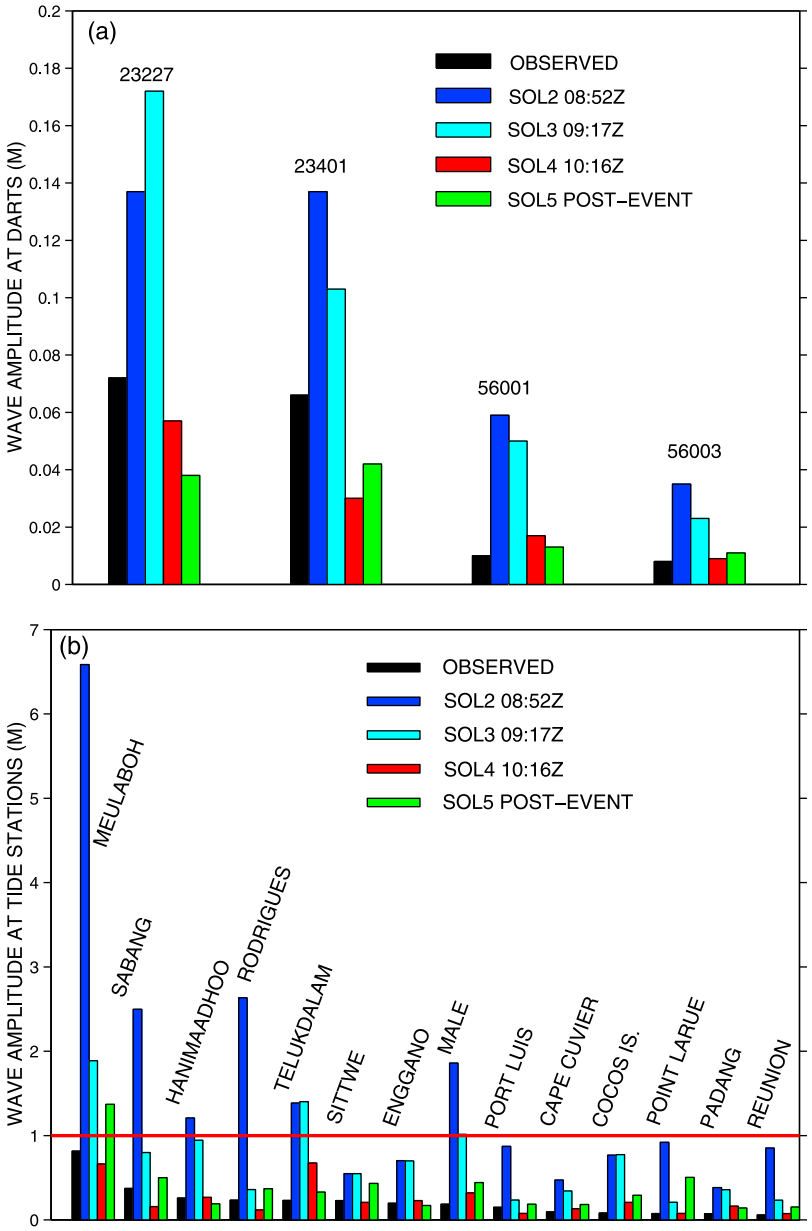

Figure 2. (a) Comparison between observed wave amplitudes at DARTs with RIFT forecast. (b) Comparison between observed wave amplitudes at tide stations with RIFT forecasts. SOL5 (in green) was a post-event run based on the USGS W-phase CMT second nodal plane (Mw = 8.57, strike = 108°, dip = 87°, and rake = 170°), included for comparison. Wave amplitude is defined as an average of maximum zero to peak and zero to trough amplitudes.

have been obtained in real-time, and the worst case scenario (SOL5) should have been chosen, for warning purposes. However, the results of SOL5 and SOL4 are rather similar qualitatively and are more accurate than the thrust scenarios, although wave amplitude of 1.37 m at Meulaboh exceeded the warning threshold, vs. the observed 0.82 m and 0.66 m from SOL4.

[15] Accurate estimate of tsunami arrival time is important for tsunami warning. The tsunami arrival times from RIFT are generally within 20–30 min. the observed, although the coastal arrival times in RIFT are inferred from the offshore points.

[16] RIFT forecast and near real-time sea-level gauge measurements would have given PTWC the confidence to cancel the tsunami watch had there been only one earthquake. However, the actual cancellation was delayed because of the second earthquake (PTWC's initial magnitude estimate was 8.3). When PTWC duty scientists were certain that the data from coastal sea-level gauges and DARTs did not show a significant tsunami for the second earthquake they cancelled the basin-wide tsunami watch at 12:36 UTC.

4. Conclusions

[17] We have developed a methodology for real-time tsunami forecasting (RIFT), using best available earthquake parameters. The RIFT model accepts any fault geometry as input and capitalizes on the recently developed W-phase method, which rapidly determines an earthquake's source parameters, including its mechanism. The RIFT forecasting

system is versatile because it generates the computation domain on the fly, accepts input of the actual focal mechanism of the earthquake, can account for both local and global domains, and can handle multiple events in different or the same ocean basins.

[18] We showed that a real-time forecast model can enhance the forecast capabilities of the tsunami warning centers. The RIFT model was run four times at PTWC during the April 11, 2012 Sumatra tsunami. These successive real-time forecasts during the event, based purely on the available earthquake parameters, improved the accuracy of the forecasts as shown by observations both at the DARTs and the sea-level stations, thereby demonstrating the importance of rapid and accurate seismic information for tsunami forecasting.

[19] **Acknowledgments.** We thank Laura Kong for her support throughout the RIFT development. We thank George Choy of USGS for helpful comments. We thank Dominique Reymond and an anonymous reviewer for their constructive comments and suggestions, which helped improve the paper.

[20] The Editor thanks Dominique Reymond and an anonymous reviewer for assisting in the evaluation of this paper.

References

Arakawa, A., and V. Lamb (1977), Computational design of the basic dynamical processes of the UCLA general circulation model, *Methods Comput. Phys.*, *17*, 174–267.

Becker, J. J., et al. (2009), Global bathymetry and elevation data at 30 arc seconds resolution: SRTM30_PLUS, *Mar. Geod.*, *32*(4), 355–371, doi:10.1080/01490410903297766.

Duputel, Z., L. Rivera, H. Kanamori, G. P. Hayes, B. Hirsorn, and S. Weinstein (2011), Real-time W-phase inversions during the 2011 Tohoku-oki earthquake, *Earth Planets Space*, *63*(7), 535–539, doi:10.5047/eps.2011.05.032.

Duputel, Z., L. Rivera, H. Kanamori, and G. H. Hayes (2012), W phase source inversion for moderate to large earthquakes (1990–2010), *Geophys. J. Int.*, *189*, 1125–1147, doi:10.1111/j.1365-246X.2012.05419.x.

Foster, J. H., B. A. Brooks, D. Wang, G. S. Carter, and M. A. Merrifield (2012), Improving tsunami warning using commercial ships, *Geophys. Res. Lett.*, *39*, L09603, doi:10.1029/2012GL051367.

Fryer, G. J., N. D. Holschuh, D. Wang, and N. Becker (2010), Improving tsunami warning with a rapid linear model, Abstract NH33A-1378 presented at 2010 Fall Meeting, AGU, San Francisco, Calif., 13–17 Dec.

Geist, E. L. (2005), Rapid tsunami models and earthquake source parameters: Far-field and local applications, *ISET J. Earthquake Technol.*, *42*, 127–136.

Geist, E. L., and R. Dmowska (1999), Local tsunamis and distributed slip at the source, *Pure Appl. Geophys.*, *154*, 485–512, doi:10.1007/s000240050241.

Gica, E., V. T. M. C. Spillane, C. Chamberlin, and J. Newman (2008), Development of the forecast propagation database for NOAA's Short-term Inundation Forecast for Tsunamis (SIFT), *NOAA Tech. Memo. OAR PMEL-139*, 95 pp., Pac. Mar. Environ. Lab., Seattle, Wash.

Hayes, G. P., L. Rivera, and H. Kanamori (2009), Source inversion of W phase: Real-time implementation and extension to low magnitudes, *Seismol. Res. Lett.*, *80*(5), 817–822, doi:10.1785/gssrl.80.5.817.

Henry, C., and S. Das (2001), Aftershock zones of large shallow earthquakes: Fault dimensions, aftershock area expansion and scaling relations, *Geophys. J. Int.*, *147*, 272–293, doi:10.1046/j.1365-246X.2001.00522.x.

Imamura, F. (1996), Review of tsunami simulation with a finite difference method, in *Long-Wave Runup Models*, edited by H. Yeh, P. Liu, and C. Synolakis, pp. 25–42, World Sci., Singapore.

Kamigaichi, O. (2009), Tsunami forecasting and warning, in *Encyclopedia of Complexity and Systems Science*, edited by R. A. Meyers, pp. 9592–9618, Springer, Heidelberg, Germany.

Kanamori, H., and L. Rivera (2008), Source inversion of W phase: Speeding up seismic tsunami warning, *Geophys. J. Int.*, *175*, 222–238, doi:10.1111/j.1365-246X.2008.03887.x.

Kowalik, Z., and P. M. Whitmore (1991), An investigation of two tsunamis recorded at Adak, Alaska, *Sci. Tsunami Hazards*, *9*, 67–84.

Kowalik, Z., W. Knight, and T. Logan (2005), Numerical modeling of the global tsunami: Indonesian Tsunami of 26 December 2004, *Sci. Tsunami Hazards*, *23*(1), 40–46.

Lamb, H. (1932), *Hydrodynamics*, 6th ed., Dover, New York.

Okada, Y. (1985), Surface deformation due to shear and tensile faults in a half space, *Bull. Seismol. Soc. Am.*, *75*, 1135–1154.

Reymond, D., E. A. Okal, H. Hebert, and M. Bourdet (2012), Rapid forecast of tsunami wave heights from a database of pre-computed simulations, and application during the 2011 Tohoku tsunami in French Polynesia, *Geophys. Res. Lett.*, *39*, L11603, doi:10.1029/2012GL051640.

Tatehata, H. (1997), The new tsunami warning system of the Japan Meteorological Agency, in *Perspectives on Tsunami Hazard Reduction*, edited by G. Hebenstreit, pp. 175–188, Kluwer, Dordrecht, Netherlands.

Wang, D., D. Walsh, N. Becker, and G. Fryer (2009), A methodology for tsunami wave propagation forecast in real time, *Eos Trans AGU*, *90*(52), Fall Meet. Suppl., Abstract OS43A-1367.

Wei, Y., E. N. Bernard, L. Tang, R. Weiss, V. Titov, C. Moore, M. Spillane, M. Hopkins, and U. Kanoglu (2008), Real-time experimental forecast of the Peruvian tsunami of August 2007 for U.S. coastlines, *Geophys. Res. Lett.*, *35*, L04609, doi:10.1029/2007GL032250.

Wells, D. L., and K. J. Coppersmith (1994), New empirical relationships among magnitude, rupture length, rupture width, rupture area, and surface displacement, *Bull. Seismol. Soc. Am.*, *84*, 974–1002.

Wessel, P. (2009), Analysis of observed and predicted tsunami travel times for the Pacific and Indian Oceans, *Pure Appl. Geophys.*, *166*, 301–324, doi:10.1007/s00024-008-0437-2.

Wessel, P., and W. H. F. Smith (1991), Free software helps map and display data, *Eos Trans. AGU*, *72*, 441, doi:10.1029/90EO00319.